Plasma-Wall Interaction Controlled by Secondary Electron Emission

IEPC-2015-343／ISTS-2015-b-343

Presented at Joint Conference of 30th International Symposium on Space Technology and Science, 34th International Electric Propulsion Conference and 6th Nano-satellite Symposium
Hyogo-Kobe, Japan
July 4–10, 2015

Irina Schweigert*
The George Washington University, Washington DC, USA

Samuel Langendorf† and Mitchell Walker‡
Georgia Institute of Technology, Atlanta, USA

and

Michael Keidar§
The George Washington University 2, Washington DC, USA

The plasma interaction with surface made from materials with enhanced secondary electron emission is studied in kinetic simulations and in experiment. We consider the sheath formation over an emissive floating flat or grooved surfaces in a dc discharge plasma at argon low gas pressure. The discharge glow is maintained by the beam electrons emitted from a negatively-biased hot cathode. We observe different types of sheaths near the floating emissive plate and the transition between them is driven by changing the energy of beam electrons.

Nomenclature

U_0 = cathode voltage
$f_{e,i}$ = electron/ion distribution function
$v_{e,i}$ = electron/ion velocity
$J_{e,i}$ = electron/ion collisional integral
j = thermoemission electron current from cathode
j_{be} = current of beam electrons from plasma
j_{pe} = current of electrons from plasma
j_i = ion current
j_{es} = current of secondary electrons from plate
j_{esr} = current of secondary electrons returning back to the plate
ϕ = electrical potential
ϕ_s = floating plate potential
$\Delta\phi_s$ = plate potential drop
$\Delta\phi_d$ = virtual cathode dip

*Researcher, Mechanical and Aerospace Engineering Depatment, ivschweigert@email.gwu.edu
†Graduate Research Assistant, Aerospace Engineering, slangendorf3@gatech.edu
‡Associate Professor, Aerospace Engineering, mitchell.walker@ae.gatech.edu
§Professor, Mechanical and Aerospace Engineering Depatment, keidar@gwu.edu

I. Introduction

The plasma-wall interaction is the fundamental process determining plasma properties in bounded plasmas. Materials with enhanced secondary electron emission (SEE) used for manufacturing electrodes and walls in discharge chambers change the classical concept of the Debye sheath, screening plasma from the surface [1-8].

The recent studies consider an interaction of an emissive wall with (i) Maxwellian plasma and (ii) non-Maxwellian plasma with a high-energy beam. For Maxwellian plasma-wall interaction the classical theory of Hobbs and Wesson [1] indicates the potential drop of $\sim T_e$ over the emissive wall sheath and the existence of a space charge limited (SCL) regime for sheaths. The theory predicts that the SCL occurs at a wall electron yield close to unity. Further increase of wall emission creates a non-monotonic potential dip structure, repelling the additional electrons back to the wall surface. This accounts for the space charge limited name of the sheath, and the potential dip structure has been referred to as a virtual cathode. In 1988, Intrator et al. [9] measured sheaths over a thermionically emitting grid using emissive probes. The results showed a profile similar to the Hobbs and Wesson prediction, with a virtual cathode. The authors questioned how such a structure could be stable, reasoning that slow ions would become trapped in the potential dip and neutralize it. The conclusion was that ions were transported away out of the plane of the sheath, a process which was called ion pumping. In support of this conclusion, they saw that if additional neutral pressure was present, the potential dip of the virtual cathode was increasingly filled and disappeared.

A emissive surface with macroscopic features, such as periodical grooves, can enhance the effect of accumulation of the secondary electrons. Experiments with a forest of carbon nanotubes aligned normal to the surface [10] have shown very low SEE at high plasma energies, indicating that the emitted electrons are geometrically being trapped near the surface .

In this paper we present the results of experimental and theoretical study of sheath formation near emissive surface in plasma with an electron beam. We consider plasma interaction with two types of surfaces which are flat and grooved.

This paper is organized as follows. The experimental setup is described in section II. The kinetic model for the 2D description of the DC discharge is given in section III. The three types of sheaths and the transition between them are described in section IV. The quasisteady state of the sheath with oscillations is discussed in section V. The kinetic model and the model setup on sheath formation around grooved sample are presented in section VI. In section VII, the results of the grooved sample simulation are shown and a negative charge accumulation is shown in front of grooves. The conclusions are given in section VIII.

II. Experimental setup

In the experiment, we use a multidipole plasma device with confining cusp fields from permanent magnets (see for details [8]. The chamber has a cylindrical shape with the radius of 30.5 cm and the height of 91 cm. The aluminum walls of the chamber are grounded and have relatively low SEE yield. The DC discharge glows in argon at the pressure P=10^{-4} Torr. The discharge plasma is sustained by an electron beam emitted by a hot cathode, which is a tungsten filament. The voltage U_0 applied to the cathode ranges from -60 V to -120 V. The thermoemission electron current from the cathode j varies from 10 mA to 40 mA. The dielectric plate made from Al_2O_3 or BN is placed 40 cm apart from the cathode. The sheath structure is measured over the sheath near this plate, which is electrically isolated and being an insulator material has enhanced SEE yield. Plasma electron density and temperature are measured with a planar Langmuir probe. The sheath potential profiles are measured with a swept emissive probe. It is constructed of telescoping alumina tubing and a hairpin 0.005-inch diameter thoriated tungsten filament emissive tip. The planar probe data is found to fit well to the equation for the probe current from the primary electrons given by Hershkowitz [11], and the remaining bi-maxwellian plasma by the analysis of Knapmiller et al [12], correcting all for SEE of the tungsten probe tip using the data of Hagstrum [13].

III. Kinetic model and setup for flat surface case

In our simulations, the discharge chamber is smaller than in the experiment, $r = 20$ cm and $h = 50$ cm. The calculation cell of cylindrical chamber is shown in Fig. 1. The cathode is at z = 5.6 cm, and the plate is placed with some distance d=36.4 cm apart from the cathode. Both the cathode and the plate are disks

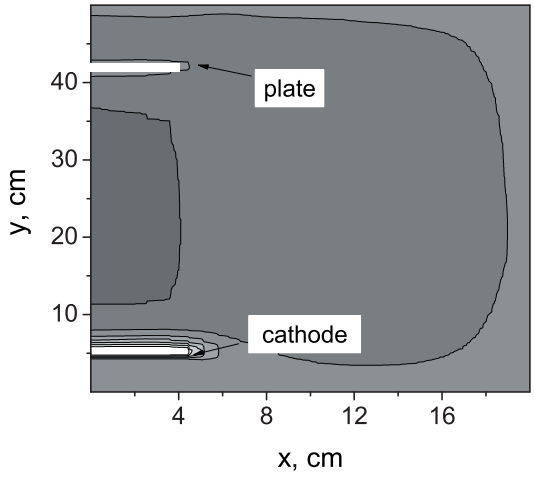

Figure 1. Electrical potential distribution for thermo-emission current j=20 mA and the cathode voltage U_0 =-70 V.

with the radii of 5 cm.

In our model, the plasma is described by the system of equations which includes the kinetic equations for electrons and ions, Poisson's equation for electrical potential and the currents balance equation for the plate floating potential. Our model is two-dimensional with cylindrical symmetry and electron and ion energy distribution functions (EEDF, IEDF) are three-dimensional in terms of velocity and two-dimensional in space (2D3V). The distribution function for electrons $f_e(\vec{r},\vec{v})$ and ions $f_i(\vec{r},\vec{v})$ are found from the Boltzmann equations

$$\frac{\partial f_e}{\partial t}+\vec{v}_e\frac{\partial f_e}{\partial \vec{r}}-\frac{e\vec{E}}{m}\frac{\partial f_e}{\partial \vec{v}_e}=J_e,\quad n_e=\int f_e d\vec{v}_e, \tag{1}$$

$$\frac{\partial f_i}{\partial t}+\vec{v}_i\frac{\partial f_i}{\partial \vec{r}}+\frac{e\vec{E}}{M}\frac{\partial f_i}{\partial \vec{v}_i}=J_i,\quad n_i=\int f_i d\vec{v}_i, \tag{2}$$

where v_e, v_i, n_e, n_i, m, and M are the electron and ion velocities, concentrations, and masses, respectively; J_e and J_i are the collisional integrals for electrons and ions with background atoms. Knowing the energy distribution functions for electrons and ions, we can calculate the mean energy of ions and electrons.

The zero-current balance equation into the surface of floating emissive plate is

$$j_{be}+j_{pe}+j_i+j_{es}+j_{esr}=0, \tag{3}$$

where j_{be} is the current of beam electrons from plasma, j_{pe} is the current of plasma electrons, j_i is the ion current, j_{es} is the current of secondary electrons emitted from the plate surface and j_{esr} is the current of secondary electrons, returning back to the surface from the virtual cathode. Poisson's equation describes the electric potential distribution

$$\triangle\phi=4\pi e(n_e-n_i),\quad \vec{E}=-\frac{d\phi}{d\vec{r}}\,. \tag{4}$$

The boundary conditions for Poisson's equation are the voltage $\phi=0$ on the grounded wall of the chamber and $\phi=U_0$ on the cathode. The floating potential of the emissive plate is calculated self-consistently from the condition of a zero total current onto the plate surface.

The discharge operates in argon. The kinetics of electrons includes elastic scattering of electrons on background atoms, excitation of metastable states, and ionization.

A. Model of secondary electron emission from the plate

In both model and experiment the flat plate is made from Al_2O_3 and the grooved plate from BN. These material have large secondary emission coefficients due to the electron bombardment γ_e, which increases

with the energy of an incident electron [14]. The electron emission is calculated by accounting for the energy distribution functions of the beam and plasma electrons. In simulation we assume that there is no secondary electron emission for electrons with the energy less than 10 eV. Secondary electrons have a Maxwellian distribution with T_e=0.1 - 0.5 eV.

IV. Three types of sheaths for emitted surface

For our experimental conditions the plasma density varies from 10^7 cm^{-3} to 5×10^8 cm^{-3}. The calculated electron density n_e distribution has a maximum value in the central part of the chamber volume. The Debye sheath forms near the non-emissive walls and there the n_e is close to zero. The potential drop over the wall sheath confines the plasma electrons. In Fig. 3, the potential distribution over the axis of symmetry is shown for different voltages and j=20 mA.

The potential drop over the cathode sheath increases with the negative bias, whereas the plasma potential slightly decreases. The electrons emitted from the hot cathode cross the sheath practically without collisions and gain the kinetic energy proportional to the potential drop. These beam electrons provide the ionization rate $\nu_i \approx 10^{13}\text{cm}^{-3}\text{s}^{-1}$ in the discharge volume for our plasma parameters.

Both in the experiment and simulation we observe a decrease of the sheath over floating emissive plate with the rise of the beam electron energy. The measured and calculated potential distribution near the plate are shown in Fig. 3 for the negative biases ranging from -60 V to -120 V. The potential profiles are given relative to the plasma potential. The computed and measured values of potential drops are in good agreement. But the measured and computed sheaths near the plate differ in size by factor of 2, because the density of plasma in simulation is smaller. A virtual cathode near the plate can be seen only on computed potential profiles in Fig. 3(b). This potential dip is created due to the excess of slow secondary electrons. No virtual cathode was observed in the experiments, which may be due to insufficient probe resolution near the wall.

A more detailed picture of modification of the potential drop near the emissive plate $\Delta\phi_s$ and the virtual cathode dip $\Delta\phi_d$ is shown in Fig. 2. We observe three types of the sheaths over the plate, and the transition between them is driven by changing the negative bias U.

Debye sheath (D) regime. First, at lower voltage $|U| < 60$ V, the classical Debye sheath similar to the cathode's and walls sheaths occurs over the plate. It is indicated by a square D in Fig. 2(a). For this case, the potential drop near the emissive plate $\Delta\phi_s = 87$ V, which is about the cathode potential drop and a virtual cathode is absent (see Fig. 2(b)). Since the $\Delta\phi_s$ is large, the beam electrons, approaching the plate, have low energy and the secondary electron emission is negligible. The beam electron current j_{be} together with the ion current j_i provide the zero-current condition on the plate.

Beam electron emission (BEE) regime. With increasing U, the transition from the Debye sheath (D) regime to the beam electron emission (BEE) regime takes place at $|U|$ =60 V. This transition is induced by switching on the secondary electron emission and accompanied by a considerable rise of the electron current from the plasma to the plate. After transition from the D regime to BEE one, the electron current to the plate rises by two orders of magnitude. Now the beam electron flux from the plasma and the secondary electron current j_{es} set the floating plate potential, $j_{be} = j_{es} - j_{esr}$, where j_{esr} is the secondary electrons, returning back to the surface by the virtual cathode. Since the plate potential drop decreases after the transition, the beam electrons approach the plate with the energy larger than 40 eV. In this case the secondary electron emission yield is $\gamma_e > 1$ and the virtual cathode appears just after the transition. With further increase of the electron beam energy (with increasing U) the potential dip of the virtual cathode becomes larger, returning more secondaries back to the surface. This increase of the potential dip helps the BEE regime to survive for some range of voltage.

Plasma electron emission (PEE) regime. The second transition is smooth and happens at U$\approx$ 90 V for the discharge current ranged from 10 mA to 40 mA. It is clearly indicated in Fig.2 by a faster decrease of the plate potential drop and shrinking the virtual cathode. The mean temperature of the plasma electrons T_e also decreases at the point of the transition. In this new regime, the cold plasma electrons start to contribute to the zero-current balance on the plate. Let us call this regime as plasma electron emission(PEE) regime. Now the currents of the cold plasma electrons j_{pe}, beam electrons j_{be} and secondary electrons, $j_{be} + j_{pe} = j_{se} + j_{ser}$ set the ϕ_s. The term j_{ser} becomes comparably small, because the virtual cathode practically disappeared (see Fig. 3(b)). Since the density of the slow plasma electrons is much larger than that of the beam electrons, a small decrease of $\Delta\phi_s$ leads to considerable increase of the plasma

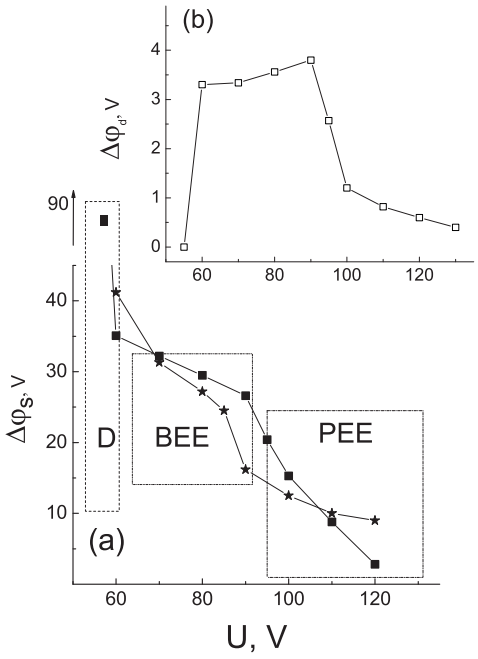

Figure 2. Potential drop over the plate sheath $\Delta\phi_s$ relative to the plasma potential for j=20 mA (squares) and j=40 mA (stars) (a) and the virtual cathode dip $\Delta\phi_d$ relative to the plate surface for j=20 mA (b). Debye sheath regime (D), electron beam emission (BEE) and plasma electron emission (PEE) regimes.

electron current. With increasing U the $\Delta\phi_s$ tends to $1T_e$.

V. Sheath oscillations near the emissive plate

The formation of a virtual cathode near the emissive wall in a Maxwellian plasma was found previously in simulations [1] and observed in the experiment [9]. In our case, the virtual cathode appears after the transition from the Debye sheath regime to BEE one. It is known that the virtual cathode appears when the total electron flux from the plasma produces a larger flux of secondaries. In Fig. 3(c), the electron and ion density profiles over the plate are shown for the Debye (U = -55 V) and BEE (U = -60 V) sheaths. In the Debye sheath, as expected, $n_i >> n_e$. The BEE sheath has a peak of plasma density near the surface with an excess of slow electrons. In simulations we use the energy dependent secondary emission coefficient, therefore the current of secondaries increases with the electron beam energy. In simulations we found that the plate sheath is in a quasistable state in the BEE and PEE regimes.

Let us consider the evolution of the potential profile during sheath oscillation cycles in our system. Note that in previous section, the figures showed the plasma parameters averaged over oscillation cycles. We found that the oscillatory behavior of the sheath near floating plate is related to the periodic accumulation of secondary electrons near the plate surface. When the negative charge of secondary electrons achieves some critical value, the plasmoid is transported to the bulk plasma. We found that the sheath oscillates in time with the frequency about 25 kHz. This frequency is set by the rate of generation of secondary electrons and the ion velocity.

Fig. 4(a) illustrates the potential distribution at different times for j=10 mA and U= - 120 V. A fragment of oscillating floating potential is shown in Fig. 4(b). The numbers in Fig. 4(b) point out the time of snapshots of the potential and electron density profiles shown in Figs. 4(a) and 4(c). During a cycle of the sheath oscillation near the plate, first, the potential bump forms (curves 1, 2 and 3) and transports the plasmoid of slow electrons to the bulk plasma. In Fig. 4(c), the electron density profiles for the same times in the oscillation cycle are shown. The plasmoid starts its motion when the floating potential starts to

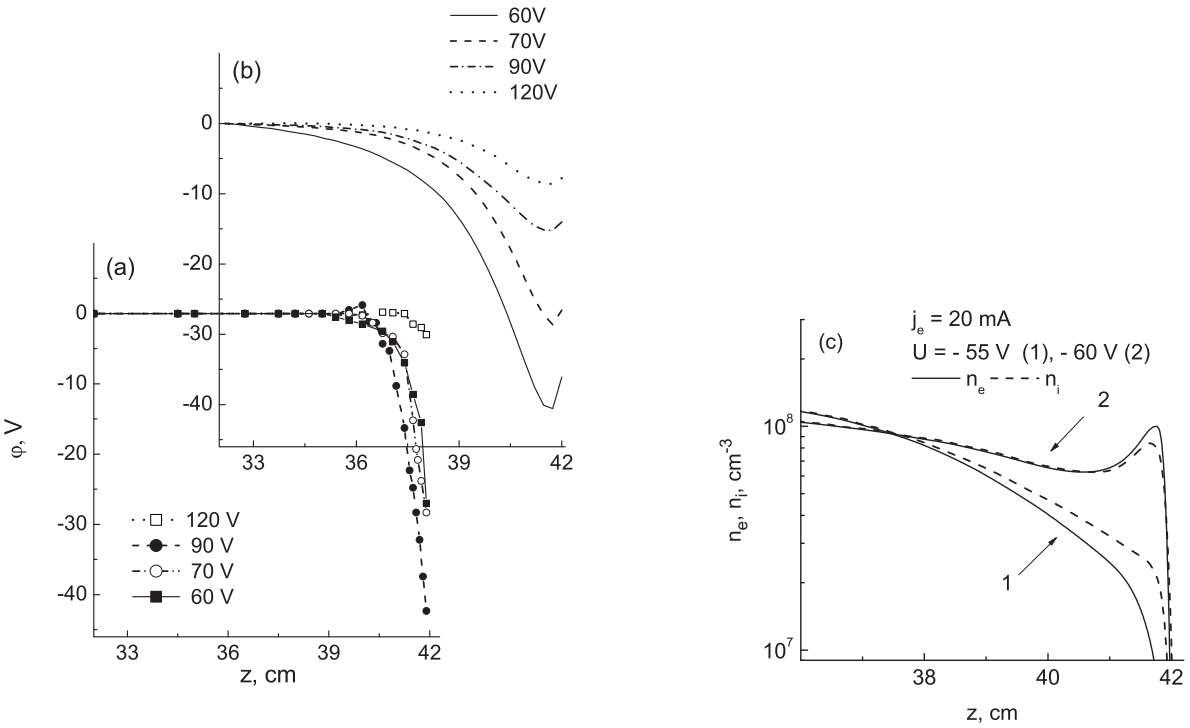

Figure 3. Measured (a) and calculated (b) potential distribution near the emissive plate for U = - 60 V, - 70 V, - 90 V and - 120 V at j=10 mA, (c) averaged electron and ion density distributions in front of the plate at r=0, for U = -55 V (1, Debye sheath) and -60 V (2, BEE sheath) at j=20 mA. Plate is at z=42 cm.

decrease. The driving potential has a maximum bump when the ϕ_s changes between points 2 and 3 (see, Fig. 4(b)). Note, that within this time interval, the potential bump value is higher than the plasma potential. As soon as the plasmoid moves away from the plate, a new one is accumulated near the surface (see curve 4 in Fig. 4(c)). The oscillation amplitude of the floating potential of the plate ranges from 2 V to 5 V, depending on the negative bias and the thermoemission current.

VI. Kinetic model and setup for grooved surface case

We consider plasma interaction with an emissive BN sample with grooves on the surface. The calculation domain is 7 cm x 5 cm plasma around this sample. The diameter of the plate is 5.5 cm and there are four 5x5 mm grooves on the surface. In Fig.7, two grooves instead of four can be seen because x=0 is a plane of symmetry. A monoenergetic electron beam enters the calculation domain from the bottom boundary. In these simulation the energy of beam electrons is 70 eV.

For accurate description of plasma dynamics inside of 5mm x 5mm grooves we developed simplified kinetic model. In experiment the sample has rectilinear grooves, therefore we solve equations (1) -(4) self-consistently in cartesian coordinates with PIC MCC method. The boundary conditions refer to a domain embedded in unlimited quasi-neutral plasma with Maxwellian electrons and ions. The electron and ion fluxes from outside are constant and given velocity distributions. The boundary conditions for Poisson's equation

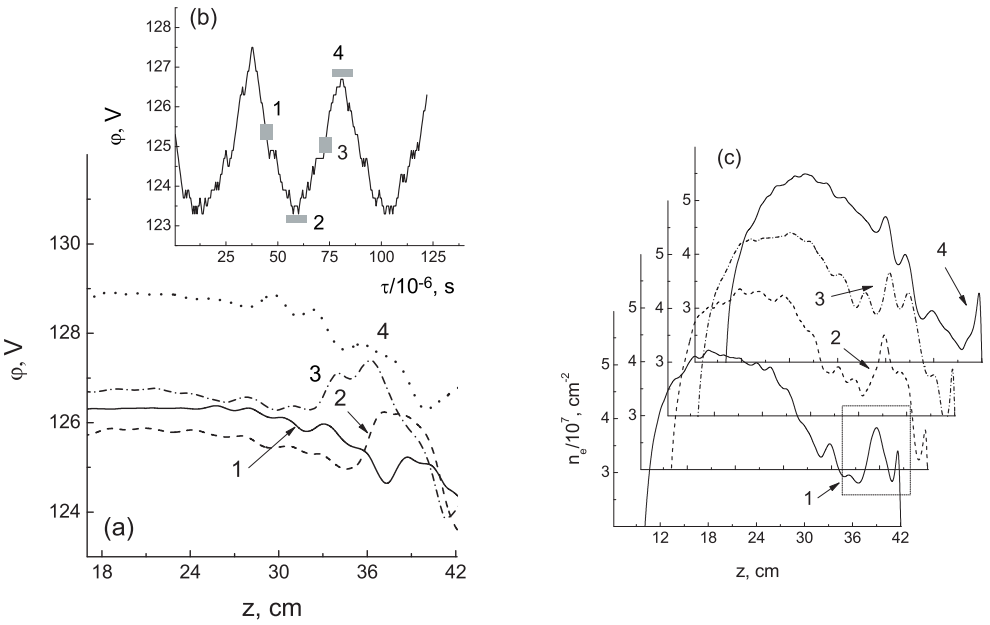

Figure 4. Electrical potential profiles at different time moments (a), fragment of floating plate potential oscillations with time (b) and electron density profiles (c) for j=10 mA, U = -120 V.

are

$$\frac{\partial \phi}{\partial y} = 0 \quad at \;\; y = 0, \qquad \frac{\partial \phi}{\partial x} = 0 \quad at \;\; x = x_{max} \; . \tag{5}$$

Initially the plasma is assumed to be a Maxwellian and quasineutral and distributed uniformly around the plate. The temperatures of Maxwellian electrons T_e=3 eV and ions T_i=0.026 eV.

The floating potential ϕ_s is calculated individually for areas 1, 2, 3, 4 (see Fig.5). The equation (3) is solved separately for fluxes of electrons from plasma, secondary electrons and ions approaching the plate surface to find ϕ_s (1), ϕ_s (2), ϕ_s (3), ϕ_s (4).

VII. Negative charge near grooved surface

Fig.5 shows the electron density distribution around the grooved plate. It is seen that the electron density is depleted within the sheath and increases near the entrance to the groove. Secondary electrons emitted inside of a groove have a Maxwellian distribution with the mean temperature of 0.5 eV and isotropic angular distribution. These electrons are trapped by the potential inside of the grooves. In Fig. 5, the charge $n_e - n_i$ distribution is shown. The positive charge on the bottom of groove (area 4) is accumulated and the plasma is not quasineutral.

The potential distribution near the plate is shown in Figs. 6 and 7. Zoom of the potential distribution around a groove is shown in Fig.7(a) from simulation and in Fig.7(b) from the experiment for the beam electron energy of 70 eV and current of 100 mA. The experimental measurement was done over y area equal 0.6 cm 0.1 cm apart from the surface. For comparison the results of experiment and calculation is shown with similar scale from 40 V to 76.6 V and are in surprisingly good agreement.

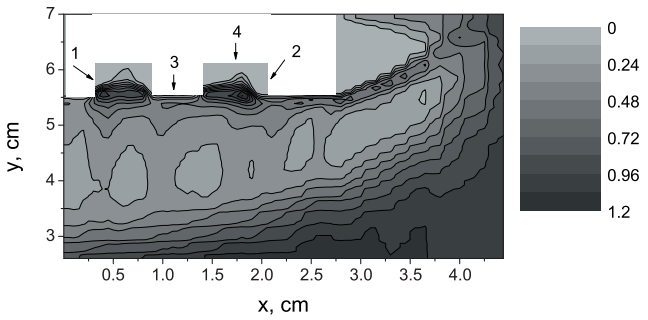

Figure 5. Electron density distribution around grooved surface measured in 10^8 cm^{-3}. Arrows show areas for definition of floating potential with equation (3).

VIII. Conclusion

In 2D3V PIC MCC simulations and in the experiment we have studied the sheath formation over an emissive floating plate with flat and grooved surfaces in a DC discharge plasma. The discharge operation in argon at P = 10^{-4} Torr is maintained by the beam electrons emitted from a negatively-biased hot cathode. The emissive plate made from Al_2O_3 or BN materials has an enhanced electron yield and is placed some distance in front of the hot cathode. We calculated the secondary electron emission by accounting for the energy distribution functions of the electrons approaching the plate surface. For the flat plate, three types of the sheaths have been found near the floating emissive plate and the transition between them was driven by changing the negative bias from -55 V to -120 V. First *the Debye sheath* appears near the plate at lower voltages at $|U|$ <60 V, when the secondary electron emission is negligible. With increasing U, the beam electrons bombard the plate with higher energy and the secondary electron emission switches on. It is accompanied with an abrupt potential decrease over the plate sheath and the increase of electron current into the plate by two orders of magnitude. This is a transition between the Debye sheath and a new sheath of *beam electron emission (BEE)* type. For the first time we have found this specific regime of sheath operation near the floating emissive surface. In this regime, the ratio of the potential drop over the plate sheath to the temperature of plasma electrons is $\Delta\phi_s/T_e$=4÷5. The floating potential of the plate is controlled by the beam electron current from plasma j_{be} and secondary electron current from the plate j_{es}, $j_{be} + j_{esr} = j_{es}$. The virtual cathode appears and helps to maintain the BEE regime within some voltage range from -60 V to -90 V. The virtual cathode modification changes the backscattering electron current j_{esr}. Further increase of U initiates the smooth transition to *the plasma electron emission (PEE)* sheath regime. In this regime, the ratio $\Delta\phi_s/T_e$ tends to unity with increasing U and the current of plasma electrons to the plate considerably increase. A variation of thermoemission current from negatively-biased cathode from 10 mA to 40 mA does not affect the qualitative picture of sheath transitions.

In PIC MCC simulations, we have also studied the oscillatory nature of the non-Debye sheath. A plasmoid of slow electrons is formed near the plate and transported to the bulk plasma periodically with frequency about 25 kHz.

In the case of grooved sample, we found excess of electrons near the grooves. In the experiment and simulation, the distortion of the electrical potential repeating the grooved surface due to the occurrence of negative charge is well visible. The sheath formation around emissive grooved surface for different plasma parameters will be studied in future work.

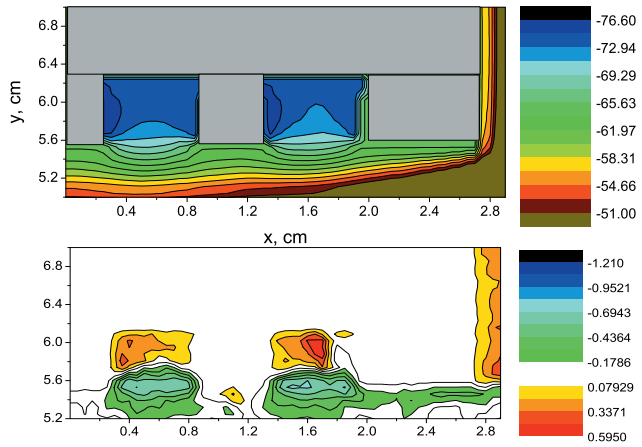

Figure 6. Potential distribution (top) and charge density ($n_e - n_i$) distribution (bottom) around grooved surface measured in 10^8 cm^{-3}.

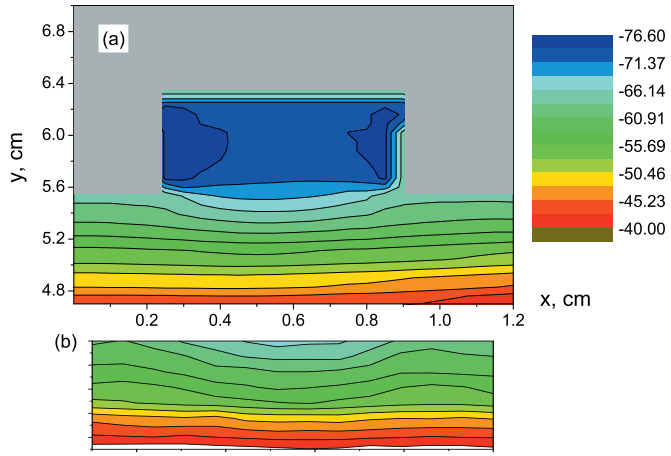

Figure 7. Electrical potential distribution around grooved surface, from calculation (a) and zoom of calculated potential (b) and from the experiment (b).

Acknowledgments

The authors gratefully acknowledge FA9550-11-1-0160, Program Manager Mitat Birkan for support of this research. One of the authors, IS, was partly supported by grant of the RFBR No 15-02-02536.

References

[1]Hobbs, G.D., and Wesson, J.A., "Heat flow through a Langmuir sheath in the presence of electron emission," *Plasma Phys.*, Vol. 9, No. 1, 1967, pp. 85, 87.

[2] Sydorenko, D., Kaganovich, I., Raitses, Y., and Smolyakov, A., "Breakdown of a Space Charge Limited Regime of a Sheath in a Weakly Collisional Plasma Bounded by Walls with Secondary Electron Emission," *Phys. Rev Lett.*, Vol. 103, No. 25, 2009, pp. 145004-1, 145004-4.

[3] Campanell, M.D., Khrabrov, A.V., and Kaganovich, I.D., "Absence of Debye sheaths due to Secondary

Electron Emission," *Phys. Rev Lett.*, Vol. 108, No. 25, 2012, pp. 255001-1, 255001-5.

[4] Campanell, M.D., Khrabrov, A.V., and Kaganovich, I.D., "General Cause of Sheath Instability Identified for Low Collisionality Plasmas in Devices with Secondary Electron Emission," *Phys. Rev Lett.*, Vol. 108, No. 23, 2012, pp. 235001-1, 235001-5.

[5] Morozov, A.I., and Savel'ev, V.V., "Kinetics of a Low-Density Plasma near a Dielectric Surface with Account for Secondary Electron Emission," *Plazma Phys. Reports*, Vol. 33, No. 1, 2007, pp. 20, 26.

[6] Keidar, M., Boyd, I.D., and Beilis, I.I., "Plasma flow and plasma-wall transition in Hall thruster channel," *Physics of Plasmas*, Vol. 8, No. 12, 2001, pp. 5315, 5322.

[7] Sheehan, J.P., Hershkowitz, N., Kaganovich, I.D., Wang, H., Raitses, Y., Barnat, E.V., Weatherford, B.R., and Sydorenko, D., "Kinetic Theory of Plasma Sheaths Surrounding Electron-Emitting Surfaces," *Phys. Rev. Lett.*, Vol. 111, No. 7, 2013, pp. 075002-1, 075002-5.

[8] Schweigert, I.V., Langendorf, S.J., Walker, M.L.R., and Keidar, M., "Sheath Structure Transition Controlled by Secondary Electron Emission," *Plasma Sources Sci. Technol.*, Vol. 24, No. 25, 2015, pp. 025012-1, 025012-4.

[9] Intrator, T., Cho, M.H., Wang, E.Y., Hershkowitz. N., Diebold, D., and DeKock, J., "The Virtual Cathode as a Transient Double Sheath," *J. Appl. Phys.*, Vol. 64, No. 6, 1988, pp. 2927, 2933.

[10] Raitses,Y., Kaganovich, I. D., and Sumant, A. V., "Electron Emission from Nano- and Micro-Engineered Materials Relevant to Electric Propulsion," IEPC-2013-390, the 33rd Int. Electric Propulsion Conference, Washington, D.C., USA, October 6 - 10, 2013.

[11] Hershkowitz, N., DeKock, J.R., Coakley, P., and Cartier, S.L., "Surface Trapping of Primary Electrons by Multidipole Magnetic Fields," *Rev. Sci. Instrum.*, Vol. 51, No. 1, 1980, pp. 64, 69.

[12] Knappmiller, S., Robertson, S., and Sternovsky, Z., "Method to Find the Electron Distribution Function from Cylindrical Probe Data," *Phys. Rev. E*, Vol. 73, No. 6, 2006, pp. 066402-1, 066402-9.

[13] Hagstrum, H.D., "Theory of Auger Ejection of Electrons from Metals by Ions," *Phys. Rev.*, Vol. 96, No. 2, 1954, pp. 325, 335.

[14] Tondu, T., Belhaj, M., and Inguimbert, V., "Electron-emission yield under electron impact of ceramics used as channel materials in Hall-effect thrusters," *J. Appl. Phys.*, Vol. 110, No. 9, 2011, pp. 093301-1, 093301-4.